Estimating Fatigue Life of Carbon-Epoxy Composites: A Rapid Method coupling Thermo-Mechanical Analysis and Residual Strength

Kilian Demilly, Jeanne Cavoit, Yann Marco, Gurvan Moreau, Guillaume Dolo, Nicolas Carrere

Author contribution statement

The authors confirm contribution to the paper as follows:

- Demilly K. : Experiments, Analysis and interpretation of results;
- Cavoit J. : Experiments, Analysis and interpretation of results;
- Marco Y. : Review and Editing, Supervision;
- Moreau G. : Review and Editing, Validation;
- Dolo G. : Review and Editing, Validation;
- Carrere N. : Methodoloy, Analysis and interpretation of results, Writting.

All authors reviewed the results and approved the final version of the manuscript.

Estimating Fatigue Life of Carbon-Epoxy Composites: A Rapid Method coupling Thermo-Mechanical Analysis and Residual Strength

Kilian Demilly[1,3], Jeanne Cavoit[1,], Yann Marco[1,], Gurvan Moreau[2,], Guillaume Dolo[3,], and Nicolas Carrere[1,*]

[1]ENSTA Bretagne, UMR CNRS 6027, IRDL, 2 rue François Verny, 29806 Brest cedex 9, France

[2]Safran Composites, 33, avenue de la Gare, 91760 Itteville, France

[3]Naval Group, Technocampus Ocean, 5 rue de L'Halbrane, 44340 Bouguenais, France

[*]Corresponding author: nicolas.carrere@ensta-bretagne.fr

Abstract: The investigation of fatigue behavior typically involves time-consuming tests, leading some researchers to explore methodologies based on self-heating tests to reduce the process. For composite materials, the conventional approach involves piecewise linear approximations of the self-heating curve and the stress transition between the first and second regimes is arbitrarily associated with a fatigue lifetime equal to 10^6 cycles. This paper proposes a novel methodology to address these simplifications. First, a non-linear viscoelastic model is used to describe the self-heating curve. Based on the mechanisms established in the literature, a link is proposed between the dissipation and the fatigue limit. The load leading to a significant contribution of non-linear mechanisms, is associated with an infinite life time. It allows the identification of an S-N curve and prediction of fatigue behavior through a minimal number of tests. The comparison with fatigue results is satisfactory.

Keywords: Polymer matrix composites, Fatigue limit, Residual strength, S-N curves, Non-deterministic analysis, Experimental technique, Intrinsic dissipation.

Nomenclature

Laminates

QI	Quasi-isotropic laminate
QI-0	Quasi-isotropic laminate with the 0^o plies in the middle plane $[-45/90/45/0]s$
QI-45	Quasi-isotropic laminate with the 45^o plies in the middle plane $[0/-45/90/45]s$
W-UD	laminate of 2D woven ply (w) and UD ply (UD) stacking sequence : $[(\pm 45)_w,(0_4)_{UD},(\pm 45)_w]$

Heat Equation

T	Temperature $[^oC]$
θ	Difference between the current temperature and the initial one $[^oC]$
Δ^*	Density of energy dissipated per cycle $[J.L^{-3}]$
f	Frequency of the cyclic or the fatigue test $[s^{-1}]$
ρ	Density $[M.L^{-3}]$
C_p	Specific Heat $[J.^oC^{-1}M-1$

Cyclic Loading

R	Stress ratio of the cyclic or the fatigue test $[N.L^{-2}]$
σ_{max}	Maximal stress applied during the cyclic or the fatigue test $[N.L^{-2}]$

Viscoelastic Model

ε	Total strain
ε^{ve}	Viscoleastic strain
ε_k^{ve}	k^{th} elementary viscoleatic strain
E	Young modulus of the laminate in the loading direction $[N.L^{-2}]$
E_r	Relaxed Young modulus of the laminate in the loading direction $[N.L^{-2}]$
τ_k	Characteristic time associated to ε_k^{ve} $[s^{-1}]$
μ_k	Weigth associated to ε_k^{ve}
$\mathcal{D}(t)$	Intrinsic dissipation $[J.L^{-3}.s^{-1}]$

S-N curve

α	Shape parameter of the Weibull distribution
β	Scale parameter of the Weibull distribution $[N.L^{-2}]$
C,S	Shape parameters of the S-N curve
σ_∞	Fatigue limit $[N.L^{-2}]$

Table 1 Nomenclature

1 — Introduction

The use of composites has increased in many industrial fields. Thanks to the high number of tests, with different monitoring systems, performed on a wide range of composite materials, the mechanisms of damage and failure under quasi-static and fatigue loading have been well known for many years (see for instance[1,2]). However, the characterisation of a given composite requires a high number of tests (standardised or not) with different stacking sequences and different environmental conditions (see the tests carried out on the AS4/8552 and IM7/8552 materials to obtain the database provided in[3]). The cost in time and money can therefore be very significant. This is particularly the case for fatigue loading. Indeed, the time needed to perform a single test could be very long (because some applications require more than 10^7 cycles and because the frequencies cannot be too high due to the self-heating observed in these materials[4]). In addition, the lifetime is highly dependent on the stress ratio[5] and the results can be highly scattered. This means that thorough fatigue characterisation of a given laminate can be very expensive and time consuming. However, it is important to note that at the material selection stage, it may be sufficient to estimate the stress leading to 10^x cycles (where x depends on the application) associated with a given confidence interval. In order to achieve this objective, a number of methods have been proposed in the literature to predict the fatigue limit with a reduced number of tests. The staircase (or up-and-down) method is one of the best known approaches to fatigue limit estimation. It consists of defining the stress amplitude applied to a specimen as a function of the result of the previous test. If the previous test failed, the stress amplitude is reduced (otherwise it is increased). A statistical method could be used to estimate the mean fatigue limit and its range of variation[6,7]. An example of this method applied to composite fatigue after impact is given in[8]. Approaches based on cyclic tests with increasing amplitude on the same specimen have also been proposed in the literature[9]. Since a progressively increasing stress amplitude is applied to the same specimen, a cumulative damage rule must be used to process the results.

Another approach is to use the rise in temperature that is observed during the cyclic tests as a marker of the fatigue mechanisms. This type of approach is called "self-heating" or "heat build-up protocol". The specimen is subjected to a series of cycles with progressively increasing mean stress (at a constant stress ratio). For each level of mean stress, the increase in temperature is recorded (using thermocouples or infrared thermography). Several authors have shown on metallic materials[10,11,12] or polymer-based materials[13,14,15,16] that the mean stress at which the temperature increases drastically could be related to the fatigue strength at 10^x (where x has to be assumed). For metallic materials, since the mechanisms responsible for the temperature increase are known, it is possible to use models to describe the self-

heating curve and the scatter of the S/N curve[11]. This is not usually the case for composites, for which the self-heating curve is usually approximated by a piecewise linear approximation (in two or three zones depending on the material). The stress corresponding to the transition between the first and second zones (or regimes) is usually associated to a fatigue life equal to 10^6 cycles. This approach has been applied to various types of polymer-based materials. However, two points can be discussed: (1) the determination of the stress at the transition and (2) the number of cycles to failure associated with this transition. To overcome these limitations a link is proposed between the dissipation determined by self-heating tests and the fatigue limit. The first section presents the material under investigation and the heat build-up test protocol. In the second section, the results of the heat build-up tests are presented. A model to describe the evolution of the intrinsic dissipation is then presented. Thanks to this model, the fatigue limit is determined on the basis of physical mechanisms described in the literature[17,18]. Finally, this fatigue limit is used to identify a probabilistic model, initially proposed by Sendckyj[19], to describe the S-N curve. The last section is dedicated to the conclusions and further work.

2 — Experimental and theoretical background

2.1 — Materials

To test the applicability of the proposed method, two carbon/epoxy materials are investigated in this article.

The first one is a quasi-isotropic laminated composite of AS7/8552 carbon/epoxy prepreg. Two stacking sequences were investigated (named after the orientation of the central layer): $[45,90,-45,0]_s$ (hereafter referred to as QI-0) and $[0,-45,90,45]s$ (hereafter referred to as QI-45). The thickness of one ply varies from 0.135 mm to 0.145 mm and the total thickness of the laminate is between 1.02 and 1.12 mm.

The second material (hereafter referred to as W-UD) is a laminate of 2D woven ply (HR fibre) and UD ply (IM fibre). The stacking sequence is $[(\pm 45)_w,(0_4)_{UD},(\pm 45)_w]$ (w stand for woven and UD stand for unidirectionnal). The thickness of the 4 UD plies is about 2/3 of the total thickness (which is equal to 3.6mm).

The two materials have been cured in an autoclave following the curing cycle recommended by the manufacturer.

2.2 — Mechanical tests and thermal measurements

The tests were carried out on an MTS servo-hydraulic testing machine. The test coupons were 250mm total length, 150mm gauge length, 25mm width (see Fig. 1). The quasi static tests were carried out at 2mm/min. The cyclic and fatigue tests were force controlled with a sinusoidal waveform. The maximum applied stress is referred

to as σ_{max} and the load ratio (minimum to maximum cyclic stress) is referred to as R. In this study, the load ratio was set to R=0.05 for the QI mterials and R=0.01 for the W-UD laminate (these were selected to meet the specific requirements of the targeted industrial applications). All tests were performed at room temperature (around 20^{o}C). For each test, an evaluation of the energy dissipated was made based on thermal measurements. (see section 2.3). The thermal imaging was carried out using an Infratec infrared camera (ImageIR 10300, 1920x1536 pixels, pixel pitch 10, μm,record frequency 100Hz, thermal resolution better than 30mK).

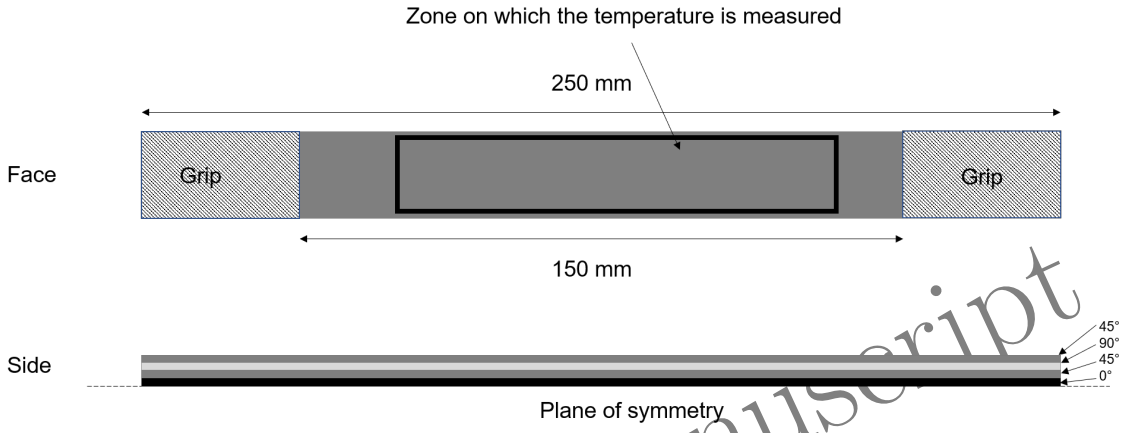

Figure 1 Geometry of the specimen

2.3 — Heat build-up protocol and determination of the cyclic dissipated energy

The heat build-up protocol consists of subjecting the specimen to a sequence of cyclic loading steps defined by a fixed stress ratio and an increasing peak stress value (see Fig. 2). This type of protocol has been applied to various composite materials (short fibre composite with thermoplastic matrix[20,21], woven composite with carbon fibres and epoxy matrix[22]) and its aim is to determine the relationship between the cyclic energy dissipated and the applied stress.

The energy dissipated during a cycle is related to the evolution of the temperature thanks to the heat equation. Under certain assumptions (not mentioned here for the sake of consistency, see for example[20,21]) including adiabaticity, the heat equation could be simplified as follows

$$\rho C_p \left.\frac{\partial \overline{\theta}(t)}{\partial t}\right|_{t\to 0} = f\overline{\Delta}^* + \overline{H}^e(t) \tag{1}$$

where ρ is the specific mass, C_p is the specific heat, θ is the difference between the current temperature and the initial temperature and f is the frequency of the cyclic loading. Δ^* is the density of energy dissipated per cycle (independent of the frequency). $\mathcal{H}^e$ is the contribution of the thermoelastic coupling on the temperature

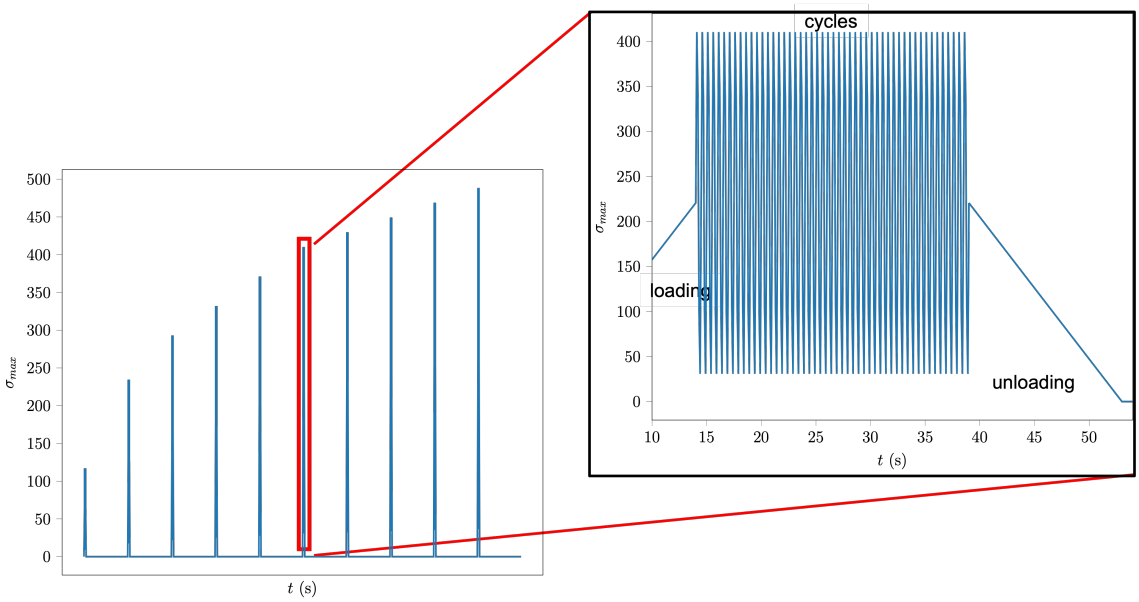

Figure 2 Example of a loading protocol

rate. The operator $\overline{x}$ stands for:

$$\overline{x} = \int_x x dS \tag{2}$$

3 — Results

3.1 — Heat-Built up tests

Heat build-up tests were carried out on the QI materials and the W-UD material. For sake of consistency, only the results of the QI materials will be discussed. In the final step, the specimen was tested until failure. The temperature change may not be uniform over the entire surface of the specimen. As the specimen moves while the camera is fixed, it is necessary to transpose each pixel in a reference configuration. This has been done using the same approach used by Navratil[22], which has been implemented in an in-house software called Celenos[23]. The evolution of the temperature as a function of time is determined at each pixel ($\theta(\vec{x}, t)$). Its spatial average over the whole gauge length is calculated ($\bar{\theta}(t)$) (an example of thermal measurement results is provided in Fig. 3). Finally, using eq. 1 is is possible to approximate the evolution of the temperature by a linear part (with a slope equal to $\Delta^*/(\rho C_p)$, see the blue line in Fig. 3) and a sinusoidal part (corresponding to thermoelastic coupling).

It is important to keep in mind that this identification is only possible if the adiabatic condition is satisfied. To ensure this, the parameters involved in eq. (1) are identified once the mechanical loading has stabilised and over a short period of time (much less than the characteristic thermal time of the specimen). For the specimens investigated (material, ply thickness, number of plies, geometry), the characteristic

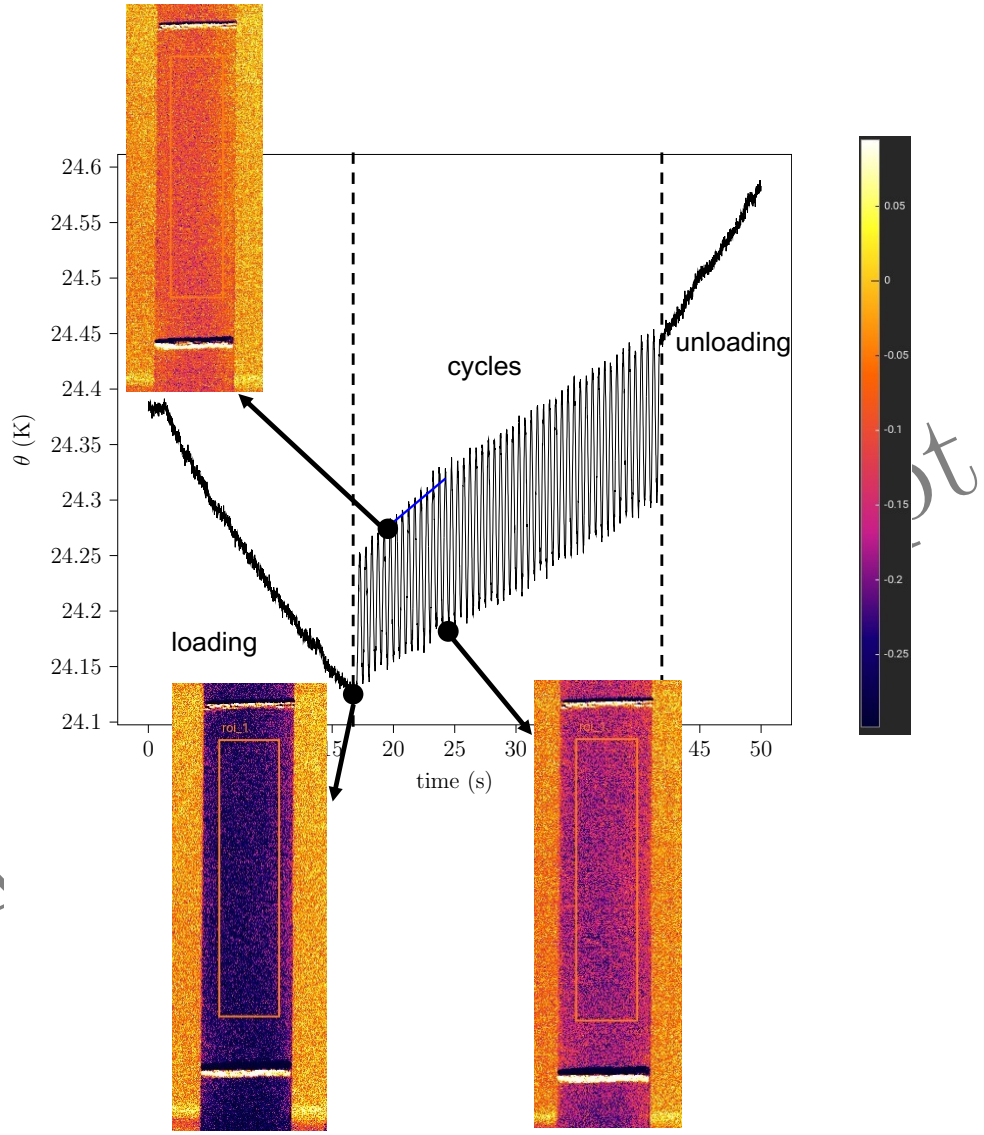

Figure 3 Evolution of the temperature on the surface of the specimen as a function of the loading. The images represent the temperature field at different moments of the cycling (end of static loading, peak of the 6th cycle, bottom of the 22nd cycle). The curve is the average temperature over the region of interest (represented by a rectangle in the temperature field images)

time was inferred to be around 65s from a cooling step (see[21]). The dissipation was identified using 10 cycles, which corresponds to a duration of 5s, much less than the characteristic time. Finally, the heat build-up curve is plotted (*i.e* the evolution of the dissipation as a function of the maximum applied stress for each loading step, see Fig. 4). Fig. 4(a) shows the results obtained on the QI-0 samples. The tests were performed at a frequency equal to 2 Hz. For test QI-0-2, some of the loading steps were performed at a frequency equal to 5 Hz. The QI-0-3 specimen was tested at 2 Hz for different applied load values than the QI-0-1 specimen. The heat build-up curves are very close for all these tests, which means that: the scatter is very small, the cyclic dissipation $\overline{\Delta}^*$ neither depends on the frequency (which is consistent with eq. 1) nor on the fatigue load history. Fig. 4(b) shows the results obtained on the QI-45 specimen. The heat build-up curves are quasi-identical to those obtained on the QI-0 specimens. This means that the cyclic dissipation obtained from the surface measurements is representative of the whole thickness of the specimen and not just the surface layer.

To confirm this experimental evaluation, transient thermal finite element modelling

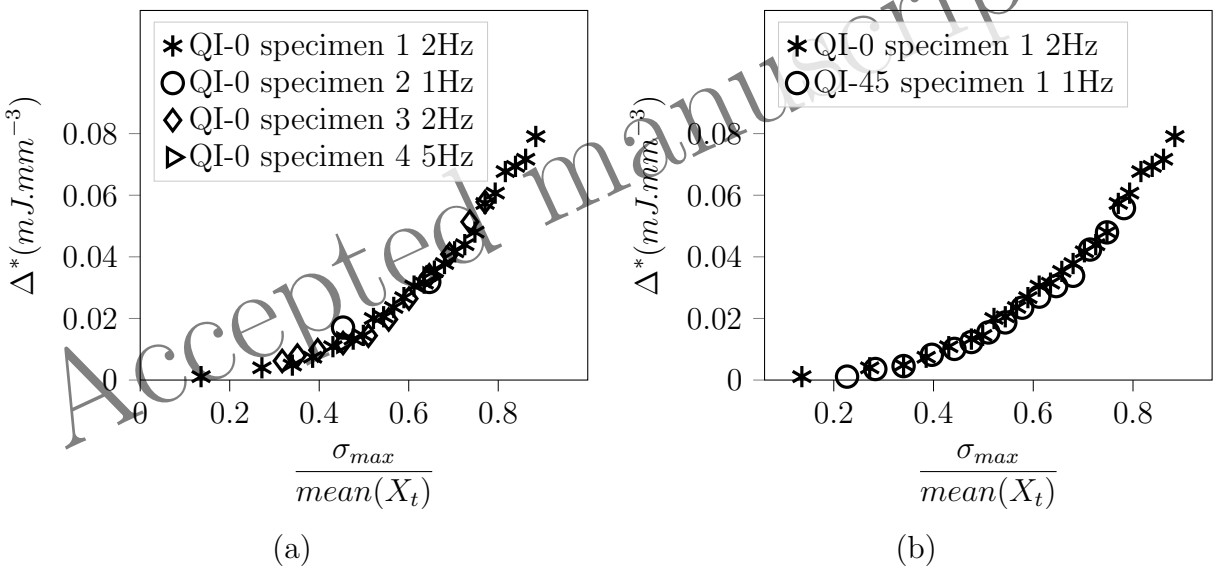

Figure 4 Heat-bulid up curves obtained from specimen oriented at 0^o (a) and 45^o (b). A result obtained on a 0^o has been reported on figure (b) to facilitate the comparison between the two orientations. The stresses applied during the loading steps have been normalized by the mean of the failure load under tensile quasi-static loading $< X_t >$.

was carried out. A half thickness was modelled using material properties from[24] (see table 2).

Four quadratic hexahedral heat trasfer fintie elemlents in the thickness of each plies have been used. No boundary conditions are applied to surfaces (symmetry bondary conditions). The heat transfer was modeled over a duration of 5 seconds, equivalent to 10 cycles for a cyclic loading at 2 Hz,this time frame is consistent with the period during which dissipation is estimated. The increase of temperature

Properties	Value
ρ $(g.cm^{-3})$	1.57
C_p $(J.g^{-1}\ ^{\circ}C^{-1})$	0.9
k_{11} $(W.m^{-1}\ ^{\circ}C^{-1})$	4.9
$k_{22} = k_{33}$ $(W.m^{-1}\ ^{\circ}C^{-1})$	0.58

Table 2 Thermal properties used for the transient thermal model (from[24])

is limited to $10^{-3}K.s^{-1}$ per increment. A constant body heat flux has been applied to each layer. Due to the difference in orientation between the different layers, the layers will not have the same level of dissipation The shear stress is the stress that leads to the highest level of dissipation, followed by the transverse stress and then the fibre direction stress (which has a very low level of dissipation)[25]. An approach aimed at calculating dissipation in each of the plies, based on a multiscale viscoelastic approach, has been developped in [26] (the detailed exploration of this approach falls outside the scope of the current article). The 0^o ply has been demonstrated to have minimal dissipation, constituting only around 20% compared to the 45^o ply. Similarly, the 90^o ply exhibits relatively low dissipation, approximately 50% compared to the 45^o ply. Therefore, the present thermal model will account for these dissipation levels in each ply (in the following, this assumption will be shown to have no effect on the result). For an applied body heat flux of $0.04mJ.s^{-1}mm^{-3}$ in the 45^o plies (which is of the order of magnitude of what is measured experimentally on the laminate, see Fig. 4) in the QI-0 laminate, the temperature rise was estimated at 0.019 $K.s^{-1}$ by the finite element calculation. Using the same approach as the one shown in eq. 1 the density of energy dissipated at the macroscopic level Δ^*_{lam} is equal to $0.027mJmm^{-3}$. It corresponds to the average of the applied applied body heat flux in each ply. The same result is obtained for the QI-45 laminate. These finite element calculations show that the macroscopic dissipation is equal to the average dissipation over the laminate thickness ($\Delta^*_{lam} = \frac{1}{t}\int_0^t \Delta^*(z)dz$). It is therefore independent of the stacking sequence and reflects the dissipation in each layer.

3.2 — Link between heat-build up curves and fatigue limit

The mechanisms leading to failure due to fatigue loading for laminates in which the failure is dominated by the fibres (hereafter referred to as fibre-dominated failure) are well known, as discussed in the work of Talreja[17] and more recently by Sørensen[18] for this class of materials. These works pointed out three types of mechanism, depending on the intensity of the stress, namely (see Fig. 5):

- at high applied stresses, fibre breakage occurs when the stress is greater than the strength of the weakest link. When a fibre breaks, decohesion can occur at the interface. Stress is transferred to the adjacent fibres. This stress transfer depends on the properties of the matrix. Number of cycles to failure is low

$(Nr < 10^3)$.

- intermediate loading will cause little or no fibre breakage (at the early stages of the fatigue lifetime). Cyclic loading can nevertheless cause cracking in the matrix. This can lead to interfacial decohesion, then fibre breakage, resulting in ply failure.

- at low applied loads, the stress is too low to cause fibre breakage or matrix cracking. It corresponds to the fatigue limit.

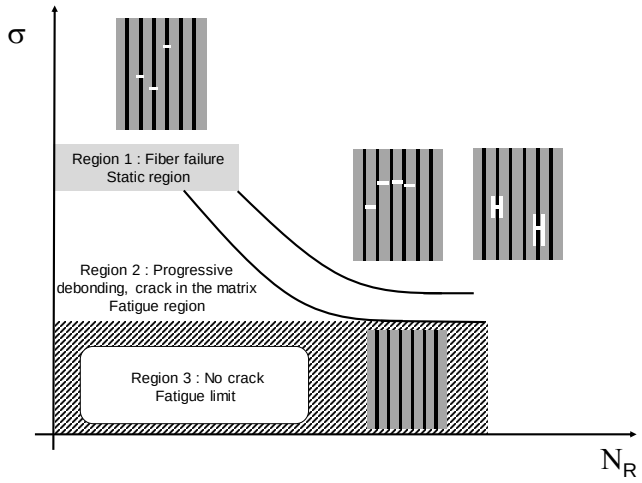

Figure 5 S-N curve (tension/tension ratio) divided into three zones: static failure, progressive fatigue failure and limit of fatigue (adapted from[2])

This description shows that it would be possible to relate the fatigue limit to the load at which the stress in the matrix is too low to cause cracking. Since the dissipation is the marker of the mechanisms occurring in the matrix, it is consistent to correlate the dissipation, estimated thanks to heat build-up tests, with the fatigue limit. Indeed, it has been shown that epoxy degradation under cyclic loading can be related to dissipation[27]. It should be possible to correlate the dissipation with the physical mechanisms involved at different scales (layer, interface) by means of an analysis combining different approaches (microscopy, acoustic emission, infrared observations, modelling...)[28 29]. It is out-of the scope of the present article and will be presented in a future work.

In this study, a model is used to determine at which level of stress the dissipation is too low to cause cracking in the matrix, this stress beeing associated to a fatigue limit as proposed by Talreja. It has been shown in the literature that the behaviour, at the ply scale or at the macroscopic scale, of this kind of material could be described by non-linear viscoelastic models[30 31].

Only the most important aspects for the understanding of the model and the calculation of the dissipation will be recalled. The model is presented for 1D loading.

The interested reader can refer to[30]. The model is written in the framework of the classical thermodynamics of irreversible processes[32]. The total strain is divided into an elastic part (ε^e) and a viscoelastic part (ε^{ve}). The free energy is assumed as follows[32]:

$$2\rho\Psi = (\varepsilon - \varepsilon^{ve}) * E * (\varepsilon - \varepsilon^{ve}) + \sum_k \frac{1}{\mu_k}\varepsilon_k^{ve} * E_r * \varepsilon_k^{ve} \tag{3}$$

where ε_k^{ve} are internal variables (strain kind) that represent elementary viscous mechanisms. E is the instanteneous Young modulus and E_r the relaxed viscous modulus. A characteristic time τ_k and a weigth μ_k (defined by a Gaussian spectrum) are associated to this viscous mechanisms. They are defined as follows:

$$\tau_k = 10^k \tag{4}$$

$$\mu_k = \frac{1}{n_0\sqrt{\pi}} exp\left(-\left(\frac{k-n_0}{n_c}\right)^2\right) \tag{5}$$

The stress is given by:

$$\sigma = \rho\frac{\partial\Psi}{\partial\varepsilon^e} = E * (\varepsilon - \varepsilon^{ve}) \tag{6}$$

Let us introduce the thermodynamic force associated to the internal variables ε^{ve} and ε_k^{ve}:

$$\begin{cases} \sigma_k^{ve} = \rho\frac{\partial\Psi}{\partial\varepsilon_k^{ve}} = \frac{1}{\mu_k}E_k * \dot{\varepsilon}_k^{ve} \\ \sigma^{ve} = \rho\frac{\partial\Psi}{\partial\varepsilon^{ve}} = -\sigma \end{cases}$$

The intrinsic dissipation is therefore given by:

$$\mathcal{D}(t) = \sigma\dot{\varepsilon}^{ve} - \sum_k \sigma_k * \dot{\varepsilon}_k^{ve} \tag{7}$$

The density of energy dissipated per cycle is calculated as follows:

$$\Delta^* = \int_t^{t+1/f} \mathcal{D}(t)dt \tag{8}$$

The evolution of the internal variables is given by the dissipation potential written as follows:

$$2\phi^* = \sum_k \frac{\mu_k}{\tau_k}(\omega_k : E_r^{-1} : \omega_k) \tag{9}$$

with $\omega_k = g\sigma^{ve} + \sigma_k^{ve}$.

It is thus possible to obtain:

$$\begin{cases} \dot{\varepsilon}_k^{ve} = -\rho\frac{\partial\phi^*}{\partial\sigma_k^{ve}} = \frac{1}{\tau_k}(\mu_k * g * E_r^{-1} * \sigma - \varepsilon_k^{ve}) \\ \dot{\varepsilon}^{ve} = g * \sum_k \dot{\varepsilon}_k^{ve} \end{cases}$$

g is a function used to describe the non-linear behavior[30]:

$$g(\sigma) = 1 + \gamma\left(\sqrt{\sigma * E_r^{-1} * \sigma}\right)^p \tag{10}$$

It is important to note that $g = 1$ corresponds to a linear model.

As explained above, the aim of the model is to evaluate the dissipation in order to determine the load at which the effect of the non-linearity on the dissipation becomes significant. To simplify the identification, classical values for carbon/epoxy are used for the parameters defining the Gaussian spectrum[31] $n_0 = 12$ and $n_c = 8$. E is the modulus in the loading direction. It can be easily estimated from monotonic tensile tests or from the properties of the ply by means of classical laminate theory. The

identification of the other parameters (E_r, γ and p) is done in two steps. In the first step, only the first part of the heat build-up curve is modelled. A linear viscoelastic model is considered ($g = 1$, *i.e.*$\gamma = 0$). It permits to identify E_r (the dot curve in the Fig. 6 is the result of this step). The non-linear function g (parameters γ and p) is identified to have a correct description of the whole curve. The results of the model from this identification is shown in Fig. 6. The non-linear model allows the heat build-up curve to be correctly reproduced, except for the high stresses at which failure mechanisms (premature fiber failure, initiation of delamination) could occur during the firsy cycles. It is possible to compare the heat dissipation obtained with a linear model with the one obtained with a non-linear model (for sake of brevity, only the results on the quasi-isotropic carbon/epoxy laminates are reported see Fig. 6). The results show that above a give stress value, the non-linear mechanisms have a significant contribution to the dissipation in comparison to the linear viscoelastic mechanisms. It therefore seems that there is a transition between a linear viscoelasticity dominated part and a non-linear viscoelasticity dominated part. It is proposed here to assume that this threshold corresponds to the fatigue limit (hereafter referred to σ_∞). This fatigue limit is related to the stress at which the dissipation predicted by the non-linear model is 5% greater than that predicted by the linear model. (5% was chosen to take account of the scatter and the accuracy of the measurements).

The stress at transition between a linear viscoelasticity dominated part and the non-linear viscoelasticity dominated part associated to the fatigue limit will be compared with fatigue results in the next section.

3.3 — Identification of a probabilistic S-N curve based on a residual strength method

Several methods have been proposed in the literature to fit results from fatigue tests (see reviews in[33,34]). Some articles have highlighted the qualities of the approach proposed by Sendeckyj[19,35]. First, it is based on strong physical considerations. Then, it has a good fitting capability and allows to associate a probability with the S-N curve. This approach is based on a residual strength model. This model describes the damage accumulation in the material as a function of the number of cycles. In this work we have chosen to use a modified version of the Sendckyj approach that has recently been proposed[36] to introduce a fatigue limit:

$$\frac{\partial \sigma_r}{\partial n} = -\gamma^{-1} C \left(\sigma_{max} - \sigma_\infty \right)^{\gamma} \left(\sigma_r - \sigma_\infty \right)^{1-\gamma} \tag{11}$$

where C anf γ and σ_∞ are parameters that must be identified and depends on the load ratio R. This equation could be integrated with the following boundary conditions: (i) at the first cycle ($n = 1$) the residual strength is equal to the equivalent static strength σ_e (*i.e.*the initial static strength of this specific specimen) and

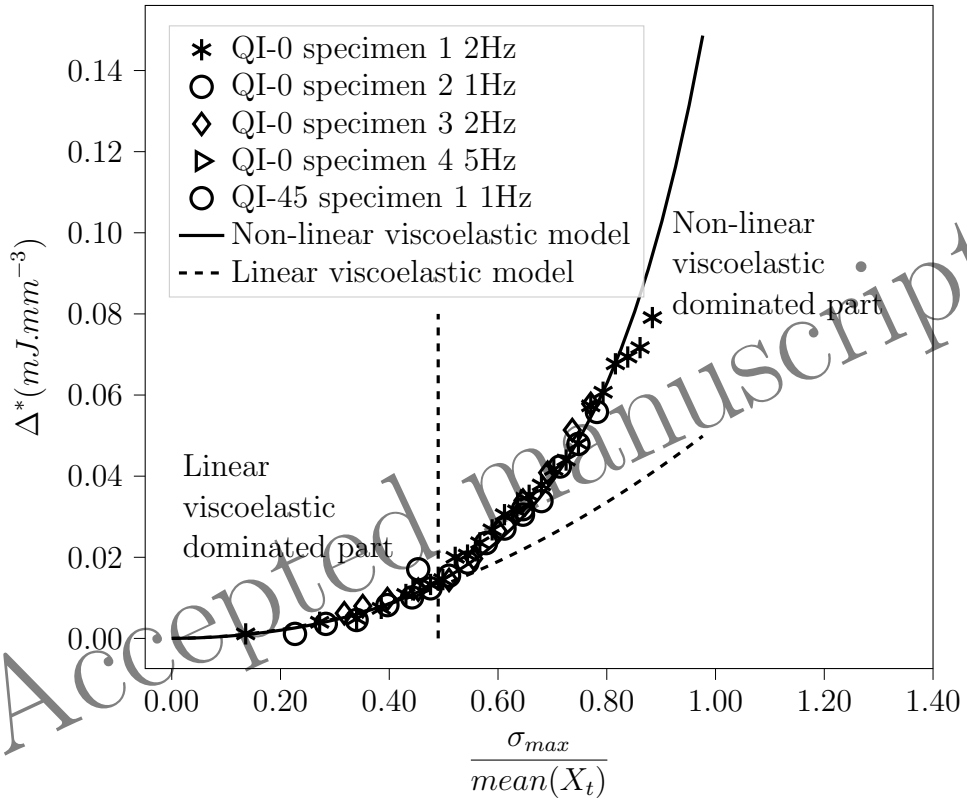

Figure 6 Heat-bulid up curves obtained on the specimens oriented at 0^o and 45^o. The dissipation predicted by the model is plotted with continuous line. The dissipation predicted by a linear visoelastic model is reported in dashed line.

(ii) failure occurs when the residual stress equals the maximum stress($n = N_R$ for $\sigma_r = \sigma_{max}$, where N_R is the number of cycle to failure). It leads to:

$$\sigma_e = (\sigma_{max} - \sigma_\infty)\Big(1 + (N_R - 1)C\Big)^S + \sigma_\infty \tag{12}$$

where $S = \frac{1}{\gamma}$. Once the parameters C, S and σ_∞ are identified, this equation allows the determination of the initial static strength (called equivalent strength by Sendeckyj) from the result of a fatigue test (pair σ_{max} and N_R) that it would have had before cyclic loading. It is important to emphasise that in order to convert results from fatigue tests to equivalent initial static strength, the damage and failure mechanisms under fatigue and static loading must be the same. A two-parameter Weibull distribution (defined by α the shape parameter and β the scale parameter) is used to describe the strength of the composite material. Finally, combining equations 12 and the Weibull distribution, the probabilistic S-N curves could be written as follows:

$$\sigma_{max} = \Big(\beta\Big[-ln\Big(P(N)\Big)\Big]^{\frac{1}{\alpha}} - \sigma_\infty\Big)\Big(C(N_R - 1) + 1\Big)^{-S} + \sigma_\infty \tag{13}$$

The mean S-N curve is given by choosing $P(N) = 0.5$. With $P(N) = 0.05$ or $P(N) = 0.95$ the S-N percentiles curves of 5% (upper bound) and 95% (lower bound) are obtained.

The identification of the parameters C, S and σ_∞ requires p_f results of fatigue tests (pair $\{N_R^i, \sigma_{max}^i\}$ for $i = 1$ to p_f) and n_s results of static tests (σ_R^j for $j = 1$ to p_s, where σ_R^j is the stress at failure obtained for the static test number p_j). Obviously, the determination of the fatigue limit requires tests with a very high number of cycles. In this paper we propose the use of the fatigue limit determined by the method presented in the previous section. Two parameters remain to be identified: C and S. A regular sampling method in the plane (C,S) has been used (see Fig. 7):

1. select values for the parameters C and S,
2. for the p_f results obtained from the fatigue tests, the equivalent strength is calculated from the eq. 12. Only low cycle fatigue tests ($10^4 > N_r > 10^2$) are used to identify the model,
3. fit a two-parameter Weibull distribution to the p_s static stresses at failure combined with the p_f equivalent strengths,
4. choose a new set of parameter C, S

The set of optimal parameters (C, S) are those leading to lowest dispersion (*i.e.* the shape parameter α of the Weibull model is maximum). The evolution of α as a function of the parameters C and S (eq. 13) is given in Fig. 8 for the quasi-isotropic material. Once the parameters identified, it thus possible to plot the probabilisitc S-N curve based on the modified Sendecyj's approach (eq. 13) (see Fig. 9 for the QI materials and Fig. 10 for the W-UD material)

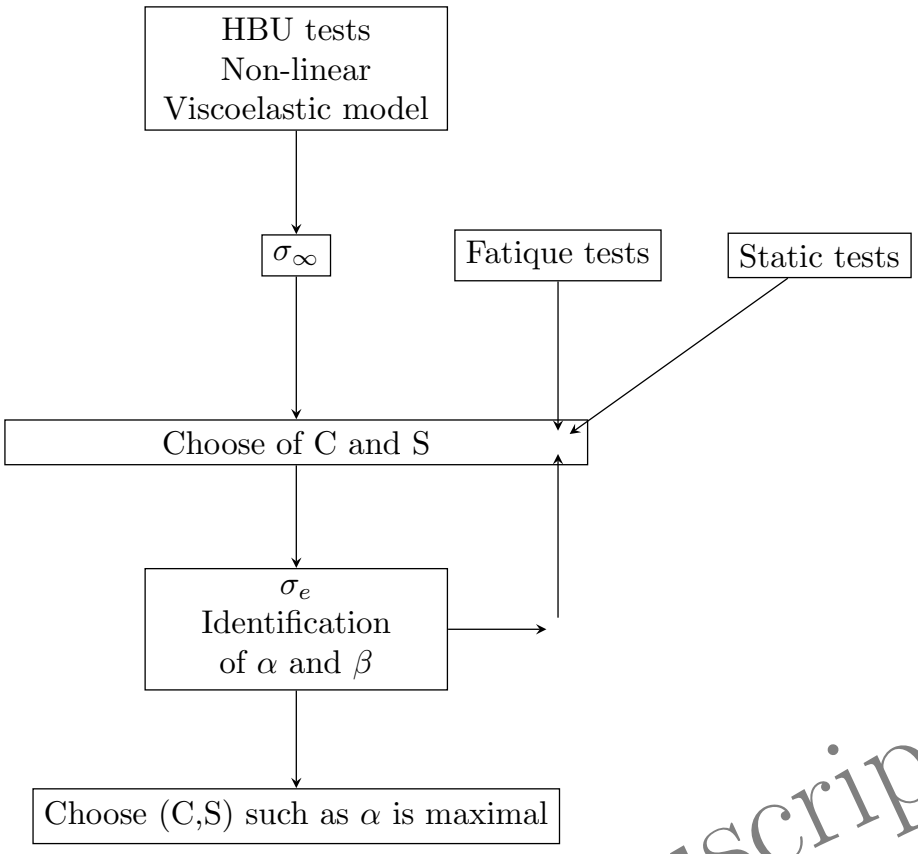

Figure 7 Algorithm used to identify the modified Sendeckyj's model

The comparison between the model results and the experimental fatigue results are quite satisfactory. Only low cycle fatigue data were used for model identification. The part of the curve corresponding to high cycle fatigue is sensitive to the fatigue limit identified thanks to the combination of the heat build-up tests and the non-linear viscoelastic model. This means that it is possible to obtain a first estimate of the fatigue limit in half a day (1 heat build-up test) and of the S-N curve in two days (10 to 15 static tests and 2-5 fatigue tests at approximately 10^4 cycles).

4 — Conclusions and perspectives

The aim of this paper was to propose a rapid methodology based on thermo- mechanical analysis, combining self-heating tests and a phenomenological modelling of dissipation. The key components of this approach include:

- the scenario proposed by Talreja for composite materials[17]. For this type of composite it has been shown that below a certain threshold (the fatigue limit) the stress in the critical plies is too low to cause fibre failure or matrix cracking,
- the use of a residual strength model. The non-deterministic S-N curve is described by an approach initially proposed by Sendeckyj[19,35]. A modified version recently proposed in[36] to introduce a fatigue limit is used,

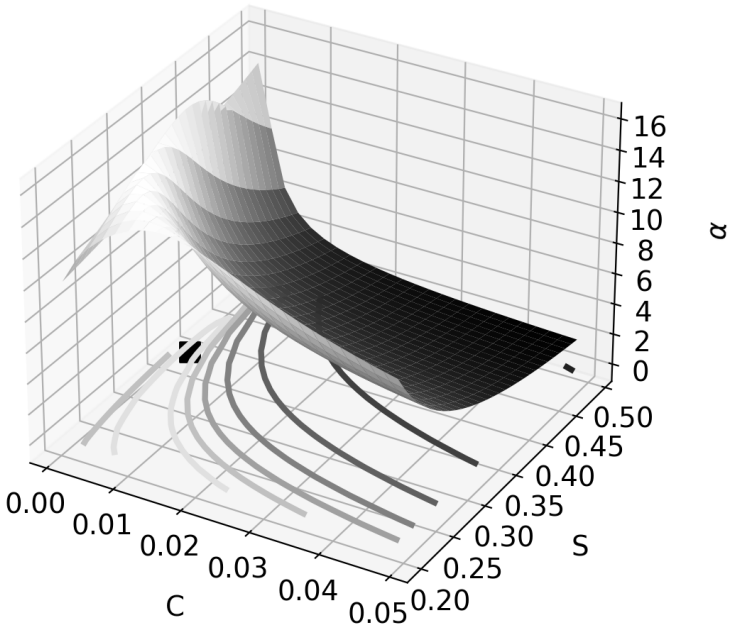

Figure 8 Evolution of the α (scale parameter of the Weibull distribution) as a function of the parameters C and S of the modified Sendecyj's approach. The black dot give the values of C and S leading to the highest value of α.

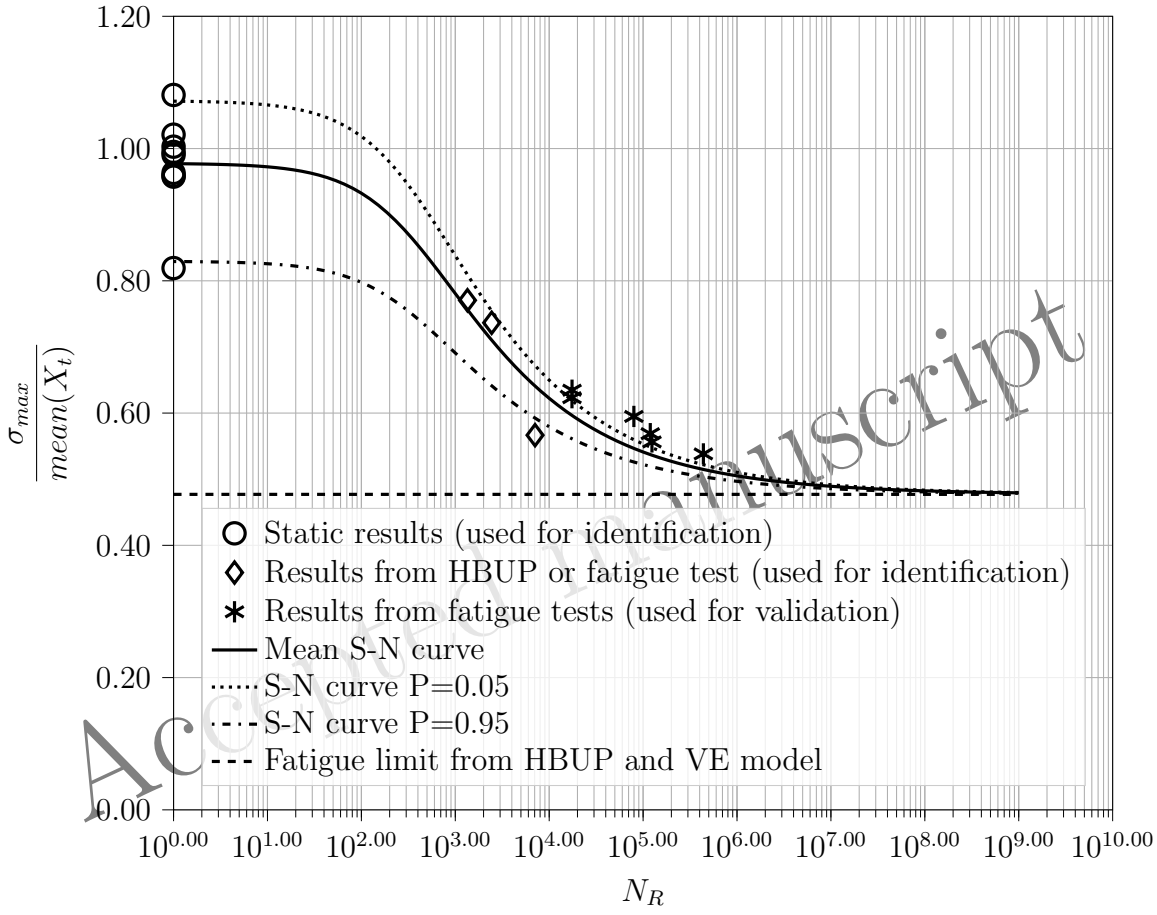

Figure 9 S-N curve predicted by the modified Sendeckyj's model on the $QI - 0$ and $QI - 45$ carbon/epoxy laminates. Only the results plotted with unfilled markers have been used for the identification. The other results are reported for comparison and validation

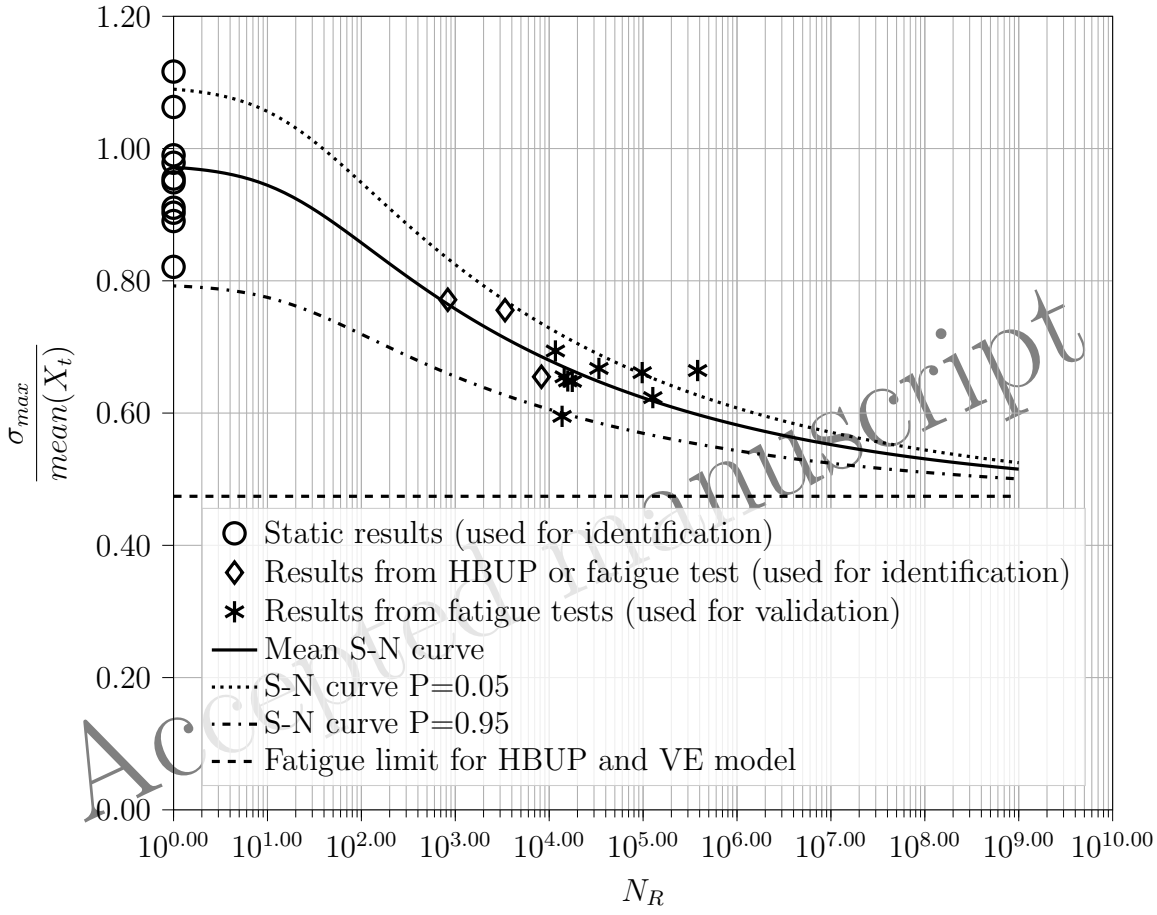

Figure 10 S-N curve predicted by the modified Sendeckyj's model on a the $[(\pm 45)_w,(0_4)_{UD},(\pm 45)_w]$ carbon/epoxy laminate. Only the results plotted with unfilled markers have been used for the identification. The other results are reported for comparison and validation

- self-heating tests for fatigue limit determination. Self-heating tests play a key role in determining the fatigue limit. Indeed, fatigue limit is the most expensive parameter to determine experimentally because it requires high cycle and very high cycle fatigue testing. The dissipation, determined from heat build-up tests, is described by a non-linear viscoelastic model. The fatigue limit is associated with stress where non-linear mechanisms become significant.

The key strength of the method presented in this article is its cost-effectiveness in the identification process. Since the fatigue limit is determined from the results of a heat build-up test, only a few tests are required to determine the S-N curve (see table 3). Some static tests are performed to identify the two-parameter Weibull distribution describing the strength and some fatigue tests (life between 10^3 and 5.10^4 cycles) to identify the parameters C and S of the S-N curve model. The results obtained with this approach are in quite good agreement with those obtained from fatigue tests on a quasi-isotropic laminate.

Type of tests	Number of repetition	Objective
1. Static up to failure	10 to 15	Young modulus (for the non-linear viscoelastic model). Probabilistic description of the strength
2. HBU test 1 (30 steps up to failure with a fixed loading increment between 2 steps and a fixed frequency)	1	Dissipation as a function of the applied load
3. Fatigue test 1 such as the failure occurs around 10^3.	1	Fatigue result 1 (σ^1_{max},N^1_R)
4. Fatigue test 2 such as the failure occurs around 5.10^3.	1	Fatigue result 2 (σ^2_{max},N^2_R)
5. Fatigue test 3 such as the failure occurs around 10^4.	1	Fatigue result 4 (σ^3_{max},N^3_R)

Table 3 Matrix of tests necessary for a quick identification of a non-deterministic S-N curve

The dissipation was described by a non-linear viscoelastic model. However, the mechanisms associated with the non-linear part of the model (function called g eq. 10 in section 3.2) are not fully understood. For this reason, it seems interesting to study in future work the mechanisms related to the increase of the dissipation of a laminated composite beyond the purely linear viscoelastic part. In order to achieve this goal, a correlation between experimental results and those obtained by a model should be used. The model should be built up from different scales at which the sources of non-linearity are progressively introduced.

Acknowledgments

This study belongs to the "Self-Heating" ANR-Safran-Naval Group research chair (Grant ANR-20-CHIN-0004) involving the Safran Companies, Naval Group, ENSTA Bretagne (IRDL) and Institut Pprime.

References

1. Reifsnider K, Henneke E, Stinchcomb W, Duke J. *Mechanics of Composite Materials - Recent advances*, chap. Damage mechanics and nde of composite laminates, Zvi Hashin and Carl T. Herakovich, Elsevier1983.

2. Talreja R. *Modern trends in composite laminated mecanis*, chap. Fatigue of Composite Materials, Altenbach A, Becker C - Springer2003.

3. K M. *Hexcel 8552 AS4 Unidirectional Material Property Data Report*, National Institute for aviation research, Whichia State University2011.

4. Sims D. *Fatigue in composites*, chap. Fatigue test methods, problems and standards, Bryan Harris, Woodhead Publish Limite2003.

5. Vassilopoulos T APand Keller. *Introduction to the Fatigue of Fiber-Reinforced Polymer Composites*, 1–65, London: Springer London2011.

6. Zhao Y, Yang B. Probabilistic measurements of the fatigue limit data from a small sampling up-and-down test method. *Int. J. Fatigue* 2008;30: 2094–2103.

7. Lin SK, Lee YL, Lu MW. Evaluation of the staircase and the accelerated test methods for fatigue limit distributions. *Int. J. Fatigue* 2001;23: 75–83.

8. Zhang J, Zhao L, Li CY M and. Evaluation of the staircase and the accelerated test methods for fatigue limit distributions. *Compos. Struct.* 2015;133: 1009–1015.

9. Rotem A. Accelerated fatigue testing method. *Int. J. Fatigue* 1981;3: 211–215.

10. Doudard C, Calloch S, Cugy P, Galtier A, Hild F. Two-scale model for high cycle fatigue life predictions. *Fatigue Fract. Eng. Mater. Struct.* 2005;28: 279–288.

11. Munier R, Doudard C, Calloch S, Weber B. Determination of high cycle fatigue properties of a wide range of steel sheet grades from self-heating measurements. *Int. J. Fatigue* 2014;63: 46–61.

12. La Rosa G, Risitano A. Thermographic methodology for rapid determination of the fatigue limit of materials and mechanical components. *Int. J. Fatigue* 2000; 22: 65–73.

13. Le Saux V, Marco Y, Calloch S, Doudard C, Charrier P. Fast evaluation of the fatigue lifetime of rubber-like materials based on a heat build-up protocol and micro-tomography measurements. *Int. J. Fatigue* 2010;32: 1582–1590.

14. Jegou L, Marco Y, Le Saux V, Calloch S. Fast prediction of the wöhler curve from heat build-up measurements on short fiber reinforced plastic. *Int. J. Fatigue* 2013;47: 259–267.

15. Kordatos E, Dassios K, Aggelis D, Matikas T. Rapid evaluation of the fatigue limit in composites using infrared lock-in thermography and acoustic emission. *Mech. Res. Commun.* 2013;54: 14–20.

16. Najd J, Harizi W, Aboura Z, Zappino E, Carrera E. Rapid estimation of the fatigue limit of smart polymer-matrix composites (pmc) using the self-heating tests. *Int. J. Fatigue* 0222;282.

17. Talreja R. Fatigue of composite materials: damage mechanisms and fatigue-life diagrams. *Proc. Royal Soc. London. A. Math. Phys. Sci.* 1981;378-1775: 461–475.

18. Sørensen B, S G. Micromechanical model for prediction of the fatigue limit for unidirectional fibre composites. *Mech. Mater.* 2019;131: 169–187.

19. Sendeckyj G. Fitting models to composite materials fatigue data. *In Test Methods and design allowables for fibrous composites . Ed. by C.C. Chamis, ASTM Intenational, USA* 1981;ASTM STP 374: 245–260.

20. Serrano L, Marco Y, Le Saux V, Robert G, Charrier P. Fast prediction of the fatigue behavior of short-fiber-reinforced thermoplastics based on heat build-up measurements: application to heterogeneous cases. *Continuum Mech. Thermodyn.* 2017;29: 1113–1133.

21. Leveuf L, Marco Y, Le Saux V, Navrátil L, Leclercq S, Olhagaray J. Fast screening of the fatigue properties of thermoplastics reinforced with short carbon fibers based on thermal measurements. *Polym. Test.* 2018;68: 19–26.

22. Navrátil L, Le Saux V, Marco Y, Aboura Z, Harizi W, Cuniberti C, et al. Understanding the damage mechanisms in 3d layer-to-layer woven composites from thermal and acoustic measurements. *J. Compos. Mater.* ;.

23. Le Seaux V. *Handbook of Celenos.* Ensta Bretagne, 2022.

24. Ulu F. *Measurement Of Multidirectional Thermal Conductivity Of Im7-G/ 8552 Unidirectional Composite Laminate*, Thesis of the North Carolina Agricultural and Technical State University2015.

25. Adams R, Bacon D. Effect of fibre orientation and laminate geometry on the dynamic properties of cfrp. *J. Compos. Mater.* 2016;7: 402–428.

26. Zimmermann de Almeida O, Cavoit J, Marco Y, Navrátil L, Moreau G, Carrere N. Study of mechanisms leading to self-heating in unidirectional laminated composites subjected to cyclic loading. *Submitt. for publication J. Theor. Comput. Appl. Mech.* ;2024.

27. Rocha I, van der Meer S FPand Raijmaekers, Lahuerta F, Nijssen RP, Sluys LJ. Numerical/experimental study of the monotonic and cyclic viscoelastic/viscoplastic/fracture behavior of an epoxy resin. *Int. J. Solids Struct.* 2019; 168: 153–165.

28. Navrátil L, Vincent LS, Leclercq S, Carrere N, Marco Y. Infrared image processing to guide the identification of damage and dissipative mechanisms in 3d layer-to-layer woven composites. *Appl. Compos. Mater.* 2022;103.

29. Palumbo D, De Finis R, Demelio P, Galietti U. A new rapid thermographic method to assess the fatigue limit in gfrp composites. *Compos. Part B* 2016; 103: 60–67.

30. Laurin F, Carrere N, Maire JF. A multiscale progressive failure approach for composite laminates based on thermodynamical viscoelastic and damage models. *Compos. Part A: Appl. Sci. Manuf.* 2007;38: 198–209.

31. Carrere N, Laurin MJF F and. Micromechanical-based hybrid mesoscopic 3D approach for non-linear progressive failure analysis of composite structures. *J. Compos. Mater.* 2012;46: 2389–2415.

32. Chaboche JL. Thermodynamic formulation of constitutive equations and application to the viscoplasticity and viscoelasticity of metals and polymers. *Int. J. Solids Struct.* 1997;34: 2239–2254.

33. Burhan I, Kim H. S-n curve models for composite materials characterisation: An evaluative review. *J. Compos. Sci.* 2018;38-2: 1–29.

34. Barbosa JF, Correia R JAFOand Freire Júnior, Zhu S, De Jesus A. Probabilistic s-n fields based on statistical distributions applied to metallic and composite materials: State of the art. *Adv. Mech. Eng.* 2019;11(8): 1–22.

35. Sendeckyj G. Life prediction for resin-matrix composite materials *Fatigue of composite materials serie 4. . K.L. Reifsnider, Ed. Elservier* 1991;431–483.

36. Angrand L. *Lois d'endommagement incrémentales pour la prévision de la durée de vie des composites tissés.* Ph.D. thesis, Paris Saclay, 2016.

Highlights

- A link is proposed between dissipation and fatigue;
- Modelling of the dissipation in laminated composites subjected to cyclic loadings;
- A criterion is proposed to identify the fatigue limit based on the dissipation;
- A S-N curve is identified and extrapolated up to high cycles fatigue.